# Gas sensing properties of tungsten oxide thin films in methane and nitric oxide gases

**P. Samarasekara**

Department of Physics, University of Peradeniya, Peradeniya, Sri Lanka

*Abstract*

*Tungsten oxide ($WO_3$) thin films, which were synthesized between micro-patterned gold electrodes and annealed at 500 $^oC$ in air for 2 hours, were developed as methane ($CH_4$) and nitric oxide (NO) gas sensors. The as-deposited films exhibited an amorphous structure and annealed films indicated crystalline $WO_3$ with the average grain size of 40 nm. The structure of films was determined by means of X-ray diffraction (XRD) methods. The highest sensitivity for 10 ppm NO gas in air at 255 $^oC$ was 0.9 and 1.6 for thin and thick $WO_3$ films, respectively. The respond and recovery times of thinner films were faster than thicker films. The sensitivity was also measured for high concentration level of methane gas for comparison. The highest methane gas sensitivity was 6.5 for 6% methane in air at 355 $^oC$. The origin of this gas sensitivity can be explained using grain boundary control model.*

## 1. Introduction

Methane ($CH_4$) is highly explosive and flammable. If halogenated chemicals are burned in the atmosphere of hydrocarbons, they recombine and produce highly toxic compounds such as dioxins and furans. Even methane mixtures of about 5% (50,000 ppm) in air are explosive. Nitric oxide (NO) gas causes slight respiratory irritation, with headache, dizziness, nausea, vomiting dyspenea, choking, burning sensation in the chest, sleeplessness, restlessness, lassitude and palpitation. Because both these gases are odorless, highly and quickly responding sensors are required to detect these gases. Therefore, researchers were motivated to detect toxic gases such as $CH_4$ and NO. Gas sensing properties of thin films of tungsten oxide ($WO_3$) films fabricated on photolithography plates were investigated in NO and $CH_4$ gases by us. The X-ray diffraction (XRD) method was used to study the structure of the films.

Tungsten based oxide gas sensor research can be summarized as following. Noble metal doped $WO_3$ thin film sensors have been synthesized by micromachining to detect $H_2S$ gas. The individual sensitivities of these Pt and the Au-Pt doped $WO_3$ gas sensors are 23 and 5.5, respectively, under 1ppm $H_2S$ and at an operating temperature of 220°C,. The response times of Pt, Au-Pt and Au doped $WO_3$ films are 30, 2 and 8s, respectively, and the recovery times are about 30, 30 and 160s, respectively [1]. Mixture of $WO_3$ and water has been formed in thick film form using sol of $WO_3 \cdot 2H_2O$ starting from $Na_2WO_4$, which differed in morphology and preferred orientation depending on the kinds and conditions of the post-treatments. According to their studies, sensor data collected at 300°C has been related with the thickness of $WO_3$ lamellas or the diameter of $WO_3$ grains, however such a relationship became less certain at 200 $^oC$ [2]. By adding oxygen plasma functionalised multi-walled carbon nanotubes (MWCNTs) to $WO_3$ and using the drop-coating deposition method, active layers for gas sensing applications have been fabricated. At different ratios of MWCNTs in $WO_3$, the response of these sensors towards toxic gases such as nitrogen dioxide, carbon monoxide and ammonia have been investigated [3]. Indium-doped nanoparticle $WO_3$ thick films, which are sensitive to $NO_2$ and CO at 200 and 300 °C, respectively, have been prepared using commercial $WO_3$ nanopowders and powder mixtures with different concentrations of indium (1.5, 3.0 and 5.0 wt %) [4].

After adding various binders such as polyvinyl alcohol (PVA), silica sol and $Al_2O_3$ to $WO_3$, the sensing and electrical characteristics of $WO_3$-based n-type semiconductor gas sensors have been investigated. According to their studies, the increase of film resistance in $NO_x$ gas mostly depends on the type of binder, and the resistance of the $WO_3$ films has indicated exponential temperature dependence in $NO_x$ gas in the temperature range of 110–375 °C [5]. $WO_2$ thin films have been

synthesized by evaporating high purity $WO_3$ powder by an electrically heated crucible on sapphire substrates provided with Pt inter-digital type sputtered electrodes and annealed for 1 h at 400, 500 and 600 °C. All the films have shown the highest sensitivity to $NO_2$ at operating temperature of 200 °C [6]. Thin film $WO_3$ micro-gas sensors have been grown by means of micro-electromechanical system technology and gas sensing characteristics have been investigated in $NO_2$. According to their studies, the $WO_3$ thin films grown at 300 °C and subsequently annealed in air at 600 °C for 4h have indicated good sensing characteristics to $NO_2$ gas at the operating temperature of 250 °C [7]. Gas sensing properties of the films of $WO_3$ and Pd have been investigated for exposure to $H_2S$ and $CH_3OH$ at operation temperatures up to 773K. These films consisting of nano-crystalline $WO_3$ and Pd have been fabricated by advanced reactive gas deposition [8].

In addition, the electrical resistance of $WO_3$ in $NO_x$ gas increases although the electrical resistance in $NH_3$, $H_2$, $H_2S$ and $SO_2$ gases decreases. These thin films of $WO_3$ have been fabricated on glass substrates by reactive radio frequency (rf) sputtering [9]. Nitric oxide gas sensitivity of $WO_3$ films grown by reactive rf sputtering method has been studied [10]. NO gas sensors have been prepared using $WO_3$ thin films synthesized by rf sputtering in various oxygen argon atmospheres. In these studies, the sputtering parameters have been optimized in order to obtain the maximum sensitivity [11]. The sensitivity of $WO_3$ thin films depends on thickness too, and $WO_3$ thin films with the thickness of 0.6 μm have indicated the highest sensitivity to $NO_2$ at 200 °C [12]. Thin film samples of various thicknesses have been fabricated by varying quantity of ammonium tungstate solution sprayed onto preheated conducting glass substrates using thermolysis technique [13]. The nano-crystalline tungsten oxide films synthesized by microfabrication technique and calcined at 550 °C for one hour have indicated the best sensitivity in $NO_2$ gas at operating temperature of 300 °C [14]. The stability of nanocrystalline $WO_3$ films fabricated using two-step thermal annealing and vacuum evaporation has been reported [15]. The XRD patterns, Raman spectroscopy, AFM measurements and optical transmission spectra of this kind of $WO_3$ films have been investigated [16].

## 2. Experimental details

Patterns of gold (Au) electrodes on thermally oxidized silicon wafers have been fabricated using photolithography and chemical etching methods. Gold layer of 100-200 nm thick was coated on one of the above substrates by vacuum evaporation. The patterns were cleaned by acetone and vacuum dried before coating of $WO_3$ thin films. $WO_3$ thin films were synthesized between micro-patterns of Au electrodes using vacuum evaporation. Some films were subsequently annealed at 500 °C in air to crystallize the phase of $WO_3$. XRD patterns were performed to investigate the structure of deposited films.

The surface resistance of the film between two gold electrodes is measured to determine the gas sensitivity, by means of a high mega Ohm multimeter. The gas sensitivity of the sample placed in a glass chamber was measured with time in a mixture of $CH_4$ or NO, and air. The sample was heated using a heater coil attached to a DC regulated power supply in order to study the variation of gas sensitivity at different temperatures. The temperature was measured using a thermocouple contacting the surface of thin film together with a digital display. Needle valves coupled to digital displays were used to control the gas flow rates entering into the measuring glass chamber. In this dynamic process, the ratio between gas flow rates passing through the chamber was controlled to vary the ratio between particular gas and air inside the chamber. Atomic Force Microscope (AFM) measurements were performed to determine the thickness of the sample and the surface morphology including the crystalline structure.

## 3. Results and Discussion

The XRD patterns of a sample prepared on glass substrates using vacuum evaporation are given in figure 1. Lower line (dashed line) and upper line (solid line) indicate XRD patterns of a sample before annealing and after annealing at 500 °C for 2 hours in air. The glass substrate does not contribute any peak to XRD pattern, and the amorphous hump can be seen around $2\theta=25^0$. The as-

deposited sample is amorphous, and the sample could be crystallized after annealing under these conditions, according to these two XRD patterns. The average grain size calculated using Scherrer's formula [16] for the first peak (002) was found to be 40 nm. All the peaks in this pattern belong to the phase of $WO_3$ [17, 18], indicating that the single phase of $WO_3$ can be crystallized under these annealing conditions. Tetragonal, orthorhombic, monoclinic and triclinic phases of $WO_3$ can be found at different temperatures [9, 18, 19, 20]. According to XRD peaks, $WO_3$ film given in figure 1. indicates properties of monoclinic phase [17, 18]. Phase of $WO_3$ at the room temperature is most probably monoclinic as given in some early publication [21, 22]. Crystallization improvement with annealing conditions of $WO_3$ thin films at temperatures 250 to 450 $^o$C has been observed by some other researchers [18]. The mechanism of crystallization improvement with annealing is related to the filling the oxygen atoms in vacant sites of crystal lattice.
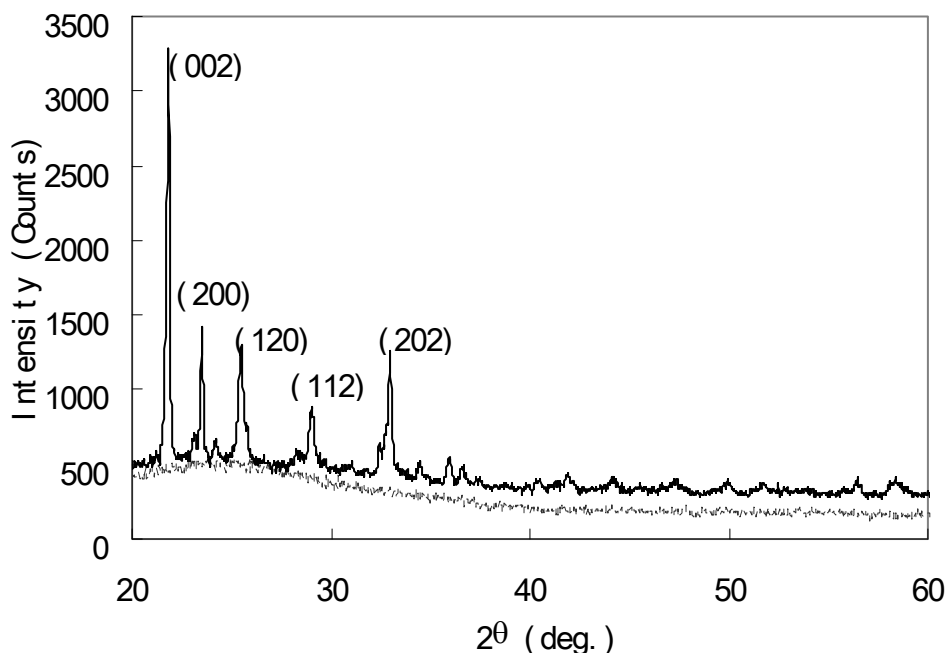


**Figure 1.** XRD patterns of a sample deposited on glass substrate before annealed (lower line) and after annealed at 500$^o$C for 2 hours in air (upper line)

Nitric oxide gas sensitivity of $WO_3$ thin films measured in NO of 10ppm at 255 $^o$C operating temperature is shown in figure 2. The thickness of this film is 55 nm as measured by AFM.
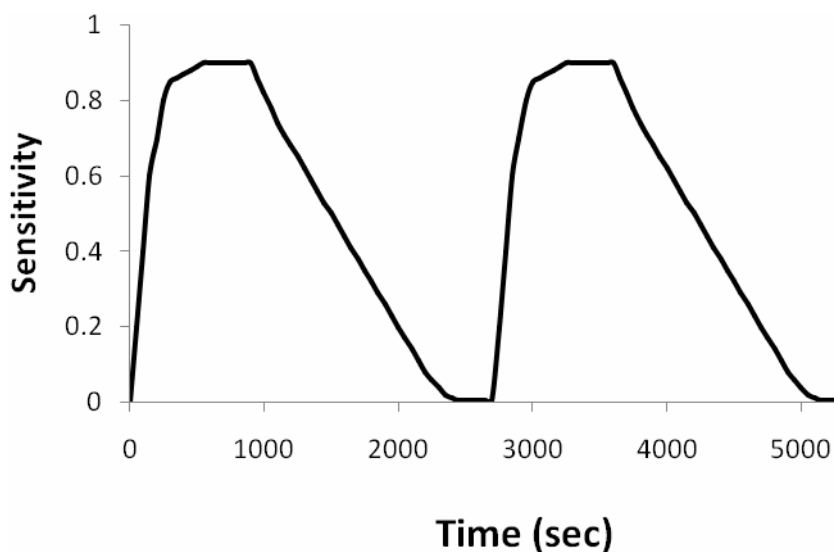


**Figure 2.** Nitric oxide gas sensitivity of $WO_3$ thin film (55nm) in a mixture of 10 ppm NO in air at 255 $^o$C operating temperature

The gas sensitivity is defined as the ratio of the difference between resistance at a particular point and initial resistance to the initial resistance. Here few curves were measured to show the repetition of data. The resistance of $WO_3$ film increased and saturated after introducing nitric oxide gas, and resistance decreased after closing nitric oxide gas flow. The maximum sensitivity is 0.9 at this operating temperature. Respond and recovery times are 550 and 1550 s, respectively.

The methane gas sensitivity percentage of $WO_3$ thin films in a mixture of methane (6%) in air at 355 $^o$C operating temperature is given in figure 3. Respond and recovery times are 3718 and 117 s, respectively. The highest sensitivity is 6.5 in this case. According to the graph, this film quickly releases methane gas.
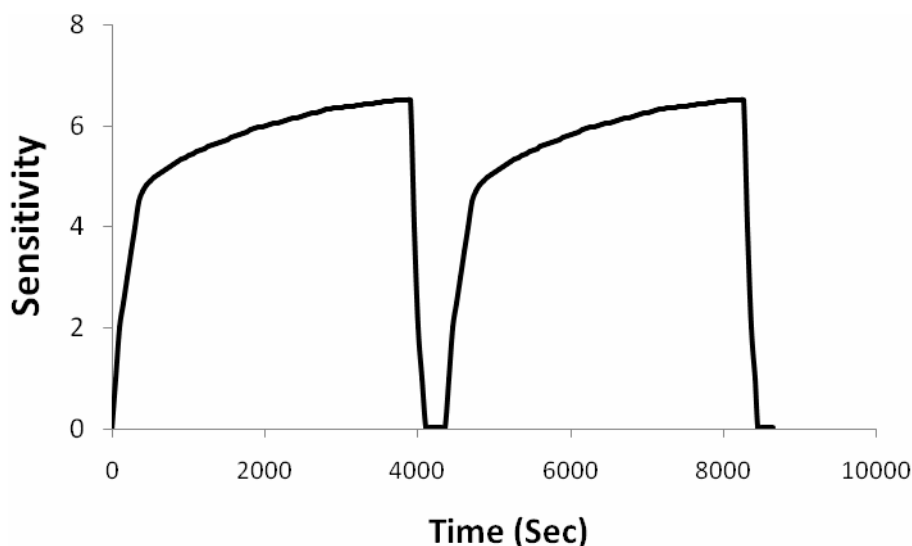


**Figure 3.** Methane gas sensitivity of $WO_3$ thin films in a mixture of methane (6%) in air at 355 $^o$C operating temperature

Figure 4 indicates the nitric oxide gas sensitivity of $WO_3$ thick films in 10 ppm NO in air measured at 255 $^o$C operating temperature. Respond and recovery times are 720 and 2920 s, respectively. Here these few curves reflect the reproducibility of our data. The thickness of this film was 110 nm. The maximum sensitivity is 1.6 at this temperature. The respond and recovery times of thin film are shorter than those of thick film. Also it was found that the maximum NO gas sensitivity of thick film is higher than that of thin film.
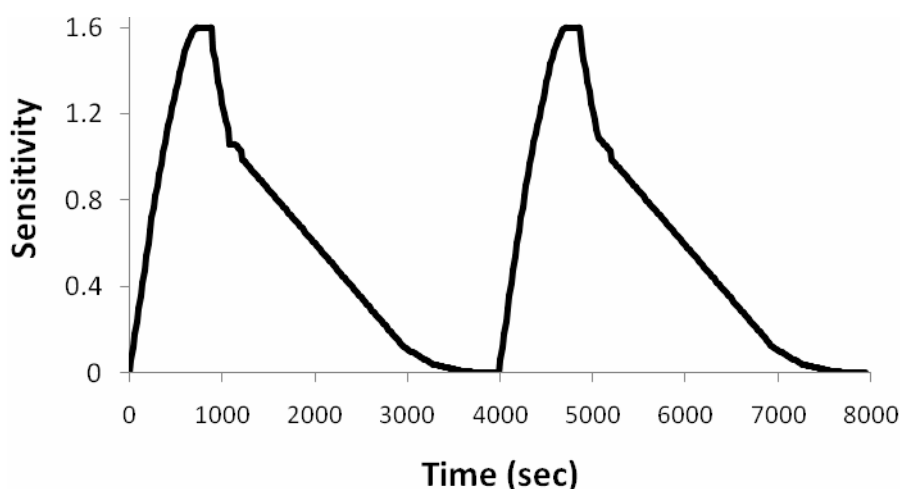


**Figure 4.** Nitric oxide gas sensitivity of $WO_3$ thick film (110nm) in a mixture of 10 ppm NO in air at 255 $^o$C operating temperature

The possible reason for this higher sensitivity is the higher effective surface area of thick film. The maximum gas sensitivity of the thick $WO_3$ samples measured at higher operating temperatures varies with time. Therefore, this sample was measured at a low operating temperature. The NO gas sensitivity of thin and thick films has been measured in operating temperature range 150-430 $^o$C. The maximum gas sensitivity is a constant at operating temperature of 255 $^o$C. Therefore, the graphs measured at 255 $^o$C are given for thin and thick films in figure 2 and 4, respectively.

$$L_D = \left( \frac{\varepsilon \varepsilon_0 kT}{ne^2} \right)^{\frac{1}{2}}$$

The Debye length $L_D$ is given by                    for a dielectric material with dielectric constant $\varepsilon$. Debye length is the distance over which significant charge separations can occur. Here $k$, $T$, $\varepsilon_0$, $n$ and $e$ are the Boltzmann's constant, sample temperature in Kelvins, permittivity of free space, electron concentration and the charge of electron. The contribution of positive charge carriers has not been taken into account, as the mobility of heavier positive charges is less than the mobility of electron. Then the calculated value of Debye length [11] at 255 $^o$C using above equation is 10.8 nm. The average grain size calculated using XRD pattern (40 nm) is larger than $2L_D$ (=21.6 nm) in our case. When the grain size is larger than $2L_D$, the gas sensitivity does not depend on grain size as the resistance arises from the grain boundaries in which the environment gases adsorb. This is called grain boundary control model. The change of electron concentration ($n$) with temperature also affects the gas sensitivity.

At operating temperature of 403 $^o$C, the sensitivity of $WO_3$ in different NO concentrations is shown in figure 5. Here points A, B, C, D and E show the points, where 3, 6, 20, 100 and 0 ppm NO concentrations in air, respectively have been introduced. According to this graph, the maximum sensitivity at 100 ppm NO is 2.3. When the amount of NO in air increases, the sensitivity, recovery time and respond time gradually increase. This implies that the higher NO concentrations increase the sensitivities, while the lower NO concentrations provide better respond and recovery times. For example, at 60 ppm of NO, the respond and recovery times are really high with gas sensitivity as high as 2.
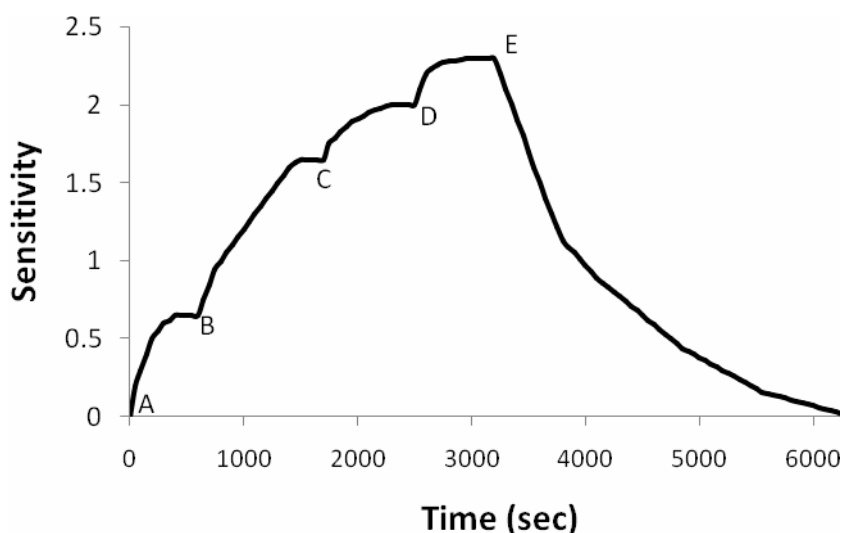


**Figure 5.** Nitric oxide gas sensitivity steps of $WO_3$ thin film at 403 $^o$C. A, B, C, D and E indicate the points, where 3, 6, 20, 100, 0 ppm of nitric oxide, respectively, were introduced. At point E, nitric oxide gas line was closed.

The maximum gas sensitivity of the thick $WO_3$ samples measured at higher operating temperatures varies with time. Figure 6 shows this effect of $WO_3$ thick film measured in 12 ppm NO at 420 $^o$C operating temperature. Sensitivities at three peaks are 0.8, 1.0 and 1.25, respectively.
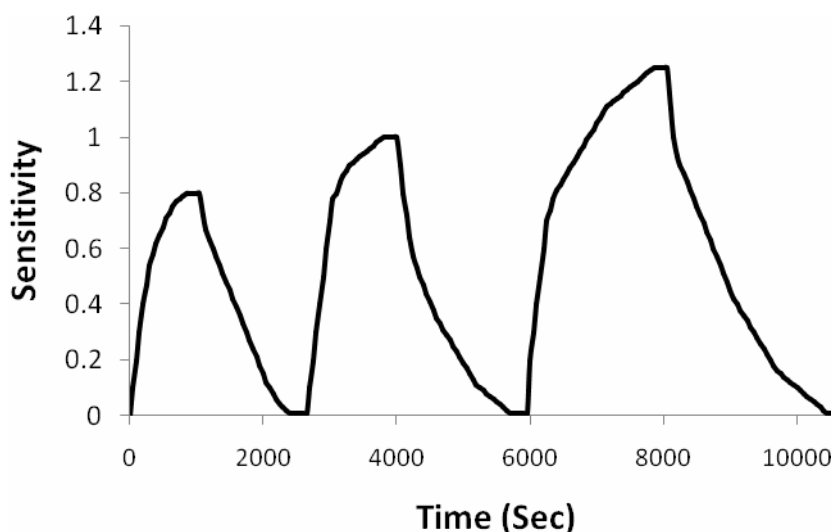
**Figure 6.** Gas sensitivity of $WO_3$ thick film measured in 12 ppm NO in air at 420 $^o$C operating Temperature

Three respond times are 850, 1120 and 1860 s, respectively. The first two recovery times are 1400 and 1760 s, respectively. This confirms that the respond and recovery times increase together with sensitivity. The reason for this effect mainly depends on following factors. The reaction taking place inside the sample during first cycle may change the phase of few crystallites inside the sample, and the new secondary phase may increase the sensitivity of the sample. If the sample does not release all the NO gas atoms absorbed by the sample in first cycle, then the maximum gas sensitivity may increase in the second consecutive cycle. Also the gas absorption may increase the effective surface area inside the sample, and the sensitivity may increase with the increase of effective surface area. It is well known that the phase of $WO_3$ changes with temperature [19, 20]. Because this effect could be specially observed at higher operating temperatures, most probably this finally explained phase change at higher temperatures can be the reason for this effect. The $WO_3$ thin films specially indicate this effect at NO concentrations above 11 ppm and operating temperatures above 410 $^o$C.

## 4. Conclusion

Only the annealed samples contribute to XRD pattern in this case. Although the sensitivity of thick films are higher than those of thin films, the respond and recovery times of thin films are better than those of thick films. The higher the $WO_3$ gas sensitivity is the higher the respond and recovery times. The highest percentage of NO gas sensitivity varies from 0.9 to 1.6, as the thickness of $WO_3$ films change from 55 to 110 nm. The maximum sensitivity varies with time at NO partial pressures above 11 ppm and operating temperatures above 410 $^o$C. Phase changes of $WO_3$ with temperature may be the possible reasons for this special effect. The highest methane gas sensitivity was measured to be 6.5 in 6% of methane in air at 355 $^o$C. However, the NO gas sensitivity of $WO_3$ films is as high as 1.6 even for very low NO concentrations (10 ppm). The Debye length ($L_D$) has been calculated to explain the mechanism behind this gas sensitivity, and the gas sensitivity does not depend on grain size because the grain boundaries adsorb gases.

**References**
1.  Wei-Han T and Ching-Hsiang T 2002 *Sensors and Actuators B Chemical* **81** 237
2.  Yong-Gyu C. Go S. Kengo S. Norio M and Noboru Y 2003 *Sensors and Actuators B Chemical* **95** 258
3.  Bittencourt C. Felten A. Espinosa E H. Ionescu R. Llobet E. Correig X and Pireaux J J 2006 *Sensors and Actuators B Chemical* **115** 33
4.  Khatko V. Llobet E. Vilanova X. Brezmes J. HubalekJ. Malysz K and Correig X 2005 *Sensors and Actuators B Chemical* **111-112** 45
5.  Jong-In Y. Lim H and Sang-Do H 1999 *Sensors and Actuators B Chemical* **60** 71
6.  Cantalini C. Sun H T. Faccio M. Pelino M. Santucci S. Lozzi L and Passacantando M 1996 *Sensors and Actuators B Chemical* **31** 81
7.  Xiuli H. Jianping L. Xiaoguang G and Wang Li 2003 *Sensors and Actuators B Chemical* **93** 463
8.  Hoel A. Reyes L F. Saukko S. Heszler P. Lantto V and Granqvist C G 2005 *Sensors and Actuators B Chemical* **105** 283
9.  Penza M. Tagliente M A. Mirenghi L. Gerardi C. Martucci C and Cassano G 1998 *Sensors and Actuators B Chemical* **B50** 9
10. Di Giulio M. Manno D. Micocci G. Serra A and Tepore A 1997 *J. Phys. D: Appl. Phys.* **30** 3211
11. Manno D. Serra A. Giulio M D. Micocci G and Tepore A 1998 *Thin solid films* **324** 44
12. Tamaki J. Hayashi A. Yamamoto Y and Matsuoka M 2003 *Sensors and Actuators B Chemical* **95** 111
13. Patil P S. Patil P R. Kamble S S and Pawar S H 2000 *solar energy materials & solar cells* **60** 143
14. Wang S H. Chou T and Liu C 2003 *Sensors and Actuators B Chemical* **94** 343
15. Jayatissa A H. Dadi A and Aoki T 2005 *Appl. Surface Sci.* **244(1-4)** 453
16. Jayatissa A H. Cheng S T and Gupta T 2004 *Mat. Sci. & Eng B.* **109(1-3)** 269
17. Abdullah S F. Radiman S. Abd. Hamid M A and Ibrahim N B 2006 *Colloids and surfaces A: physicochem Eng. Aspects* **280** 88
18. Habazaki H. Hayashi Y and Konno H 2002 *Electrochimica Acta* **47** 4181
19. Tanisaki S 1960 *J. Phys. Soc. Japan* **15** 566
20. Salje E and Viswanathan K 1975 *Acta Cryst.* **A31** 356
21. Loopstra B O and Rietveld H M 1969 *Acta Cryst.* **B25** 1420
22. Tanisaki S 1960 *J. Phys. Soc. Japan* **15** 573